

Reflection and transmission of nonlinear water waves at a semi-submerged dock

W. SULISZ

*Institute of Hydroengineering
Polish Academy of Sciences
Kościerska 7
80-328 Gdańsk, Poland
e-mail: sulisz@ibwpan.gda.pl*

A THEORETICAL APPROACH IS APPLIED TO predict reflection and transmission of nonlinear water waves at a semi-submerged dock. The solution was achieved analytically and by the method of matched eigenfunction expansions. The results show that the dock geometry has a significant effect on the nonlinear components of wave reflection and transmission. The reflection and transmission of nonlinear waves simultaneously increase with increasing dock width for shallow water waves and decrease with increasing dock width for intermediate- and deep-water waves, which is an interesting outcome. A similar simultaneous increase or decrease of nonlinear wave reflection and transmission was observed for the changes of the dock draft. Moreover, the solution reveals that nonlinear wave components may provide a significant contribution to the wave field for a wide range of wave parameters. The nonlinear components of wave reflection and transmission may exceed many times the amplitudes of the corresponding second-order Stokes waves as well as the amplitudes of the corresponding linear components. This phenomenon occurs within the commonly accepted range of the applicability of the second-order wave theory and implies a need to include scattered nonlinear wave components in the analysis of many problems of practical importance, including sediment transport, for which second-order waves have been shown to be the main driving force. Laboratory experiments were conducted to verify nonlinear wave field components. Theoretical results are in reasonable agreement with experimental data.

Key words: nonlinear waves, nonlinear diffraction, horizontal cylinder, wave-structure interactions.

Copyright © 2013 by IPPT PAN

1. Introduction

THE INTERACTION OF NONLINEAR WATER WAVES with a semi-submerged dock is of great practical importance. A large group of coastal and offshore structures are dock-like structures. Moreover, docks and decks are elements of many composite structures applied in harbor, coastal, and offshore engineering.

A first solution for the interaction of water waves with a semi-submerged dock-type structure was obtained for the interaction of long waves with a slab [1]. A more general solution to the linear diffraction or radiation problem has been achieved by employing the method of matched eigenfunction expansions [2, 3, 4]; the variational formulation of SCHWINGER [5, 6]; and numerical methods [7, 8, 9, 10]. The linear solutions obtained by applying different methods provide, in principal, the same results. The derived linear models were favorably verified by experimental data, e.g., SULISZ and JOHANSSON [11] and SULISZ [12].

Theoretical solutions to the nonlinear diffraction or radiation problem for a semi-submerged dock are rare. This is mainly related to difficulties in deriving a solution that satisfies nonlinear boundary conditions and uncertainties in theoretical descriptions of nonlinear problems. A second-order numerical approach has been applied by FALTINSEN and LØKEN [13] to calculate the mean force on a semi-submerged horizontal rectangular cylinder. SULISZ and JOHANSSON [11] derived a nonlinear analytical solution for a horizontal rectangular cylinder of substantial draft later extended by SULISZ [14] for a cylinder of arbitrary draft by applying the method of matched eigenfunction expansions. They calculated and analyzed wave loads on the cylinder and found that the nonlinear component of wave loads may be higher than corresponding first-order quantities even for waves of moderate steepness. The solution derived by SULISZ [14] was later extended to bichromatic waves by LI and WILLIAMS [15].

The solutions derived to predict nonlinear wave loads on a semi-submerged horizontal rectangular cylinder provided insight into the origin of large nonlinear wave load components on the cylinder and pointed out new aspects of nonlinear wave loads on a structure. Namely, it was shown that the nonlinear component of wave loads may be higher than corresponding first-order quantities even for waves of moderate steepness. A preliminary analysis of wave field in the vicinity of the cylinder [16] indicates that the second-order reflected waves may exceed the corresponding amplitudes of the incoming second-order Stokes waves. This phenomenon, which occurs within the commonly accepted range of the applicability of a second-order wave theory, motivated present study.

In this work, a theoretical approach is applied to predict reflection and transmission of nonlinear water waves at a semi-submerged fixed dock. The boundary-value problem is formulated up to a second-order in wave steepness and is solved analytically and by the method of matched eigenfunction expansions. The solution is analyzed with the emphasis on nonlinear components of wave reflection and transmission. Then, the laboratory experiments are described and the method to separate nonlinear components of incoming and reflected waves is presented. Finally, comparisons between theoretical results and experimental data are shown.

2. Statement of the problem

2.1. Governing equations

The situation considered for analysis is the diffraction of nonlinear long waves by a semi-submerged horizontal rectangular cylinder as shown schematically in Fig. 1. It is assumed that the sea bottom and the cylinder are impervious, and that the excitation is provided by normally incident long waves of small amplitude A_1 and frequency ω . Moreover, it is assumed that

- The fluid is inviscid and incompressible.
- The motion is irrotational.
- The sea bottom and the cylinder are impervious.

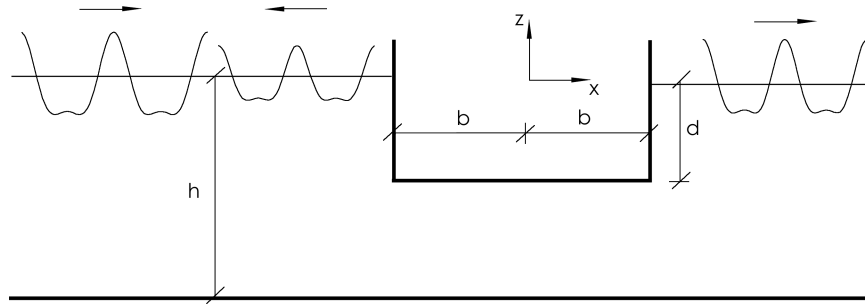


FIG. 1. Definitions sketch and coordinate systems.

According to the assumptions, the fluid velocity vector \mathbf{V} has a potential function $\Phi(x, z, t)$ such that $\mathbf{V} = \nabla\Phi(x, z, t)$. The fluid motion is governed by the classical set of equations for the irrotational motion of incompressible and inviscid fluid. Accordingly, the velocity potential must satisfy the Laplace equation

$$(2.1a) \quad \nabla^2\Phi = 0.$$

At the free surface, the velocity potential $\Phi(x, z, t)$ has to satisfy the combined free-surface boundary condition

$$(2.1b) \quad \Phi_{tt} + g\Phi_z + (|\nabla\Phi|^2)_t + \frac{1}{2}\nabla\Phi \cdot \nabla|\nabla\Phi|^2 = 0, \quad |x| \geq b, \quad z = \eta(x, t)$$

and the dynamic boundary condition

$$(2.1c) \quad \Phi_t + g\eta + \frac{1}{2}|\nabla\Phi|^2 = 0, \quad |x| \geq b, \quad z = \eta(x, t);$$

at the intersection of the dock and fluid a kinematic boundary condition must be fulfilled

$$(2.1d) \quad \Phi_z = 0, \quad |x| \leq b, \quad z = -d; \quad \Phi_x = 0, \quad |x| = b, \quad -d \leq z \leq \eta(x, t);$$

at the sea bottom the following boundary condition must be satisfied:

$$(2.1e) \quad \Phi_z = 0, \quad z = -h,$$

where ∇ is the two-dimensional vector differential operator, $\eta(x, t)$ is the free-surface elevation. Moreover, additional boundary conditions are required at infinity [17].

Once the velocity potential is known, pressure can be calculated by applying the Bernoulli equation

$$(2.2) \quad \Phi_t + \frac{1}{\rho}P + gz + \frac{1}{2}|\nabla\Phi|^2 = 0,$$

where ρ is the fluid density, P is the pressure and g is the acceleration due to gravity.

2.2. Solution technique

It is difficult to find the velocity potential and free-surface elevation which satisfy (2.1) because the free-surface boundary conditions contain nonlinear terms. Moreover, the boundary conditions must be applied on the free surface that is unknown and is a part of a final solution [18]. In order to overcome some difficulties related to (2.1), the combined free-surface boundary conditions, and the dynamic free-surface boundary conditions are expanded in a Taylor series about a mean position. The boundary-value problem can be written in the following form:

$$(2.3a) \quad \nabla^2\Phi = 0$$

with boundary conditions

$$(2.3b) \quad \Phi_{tt} + g\Phi_z + (|\nabla\Phi|^2)_t + \frac{1}{2}\nabla\Phi \cdot \nabla|\nabla\Phi|^2 + \eta \left(\Phi_{tt} + g\Phi_z + (|\nabla\Phi|^2)_t + \frac{1}{2}\nabla\Phi \cdot \nabla|\nabla\Phi|^2 \right)_z + \dots = 0, \quad |x| \geq b, \quad z = 0,$$

$$(2.3c) \quad \Phi_t + g\eta + \frac{1}{2}|\nabla\Phi|^2 + \eta \left(\Phi_t + g\eta + \frac{1}{2}|\nabla\Phi|^2 \right)_z + \dots = 0, \quad |x| \geq b, \quad z = 0,$$

$$(2.3d) \quad \Phi_z = 0, \quad |x| \leq b, \quad z = -d; \quad \Phi_x = 0, \quad |x| = b, \quad -d \leq z \leq 0,$$

$$(2.3e) \quad \Phi_z = 0, \quad z = -h.$$

Moreover, the velocity potential Φ must satisfy boundary conditions at infinity. These conditions state that a scattered potential at $x \rightarrow \pm\infty$ represents only outgoing waves.

The boundary-value problem (2.3) refers to a fixed domain, which makes it more convenient to be solved. However, the free-surface boundary conditions are still nonlinear. A solution to (2.3) can be found in the framework of weakly nonlinear wave theory by means of a perturbation procedure that has been shown to be an efficient method to deal with water-wave problems [1, 17]. The method assumes that the quantities Φ and η are expanded in powers of wave steepness

$$(2.4) \quad \begin{aligned} \Phi(x, z, t) &= {}_1\Phi + {}_2\Phi + \dots, \\ \eta(x, t) &= {}_1\eta + {}_2\eta + \dots, \end{aligned}$$

in which a quantity with a left subscript n , $n = 1, 2, \dots$ is of the order of $(A_1 k_1)^n$ where k_1 is the incident wave number and $A_1 k_1 / \pi$ is the wave steepness.

The substitution of Eq. (2.4) to Eq. (2.3) leads to the sequence of linear boundary-value problems for successive order of wave steepness. The solution of this set of boundary-value problems provides velocity potential and free-surface elevations.

3. Wave field components

3.1. Near-field components

It is straightforward to derive the linear components of the velocity potential and free-surface elevation from (2.3) and (2.4). The velocity potential and the free-surface elevation can be expressed in simple analytical forms. Further simplifications are possible by introducing complex-valued spatial functions and separating time-dependent factor. Accordingly, the wave field components can be expressed as real parts of the following expressions in brackets:

$$(3.1) \quad \begin{aligned} {}_1\Phi(x, z, t) &= \text{Re}[{}_1\phi(x, z)e^{-i\omega t}], \\ {}_1\eta(x, t) &= \text{Re}[{}_1\zeta(x)e^{-i\omega t}], \end{aligned}$$

where the quantities in brackets are complex-valued spatial functions and $i = \sqrt{-1}$.

The spatial wave-field components may be written in the following form:

$$(3.2a) \quad \begin{aligned} {}_1\phi = & -\frac{ig}{\omega} A_1 \frac{\cos \alpha_{11}(z+h)}{\cos \alpha_{11}h} e^{-\alpha_{11}(x+b)} \\ & - \frac{ig}{\omega} \sum_{m=1}^{\infty} R_{1m} \frac{\cos \alpha_{1m}(z+h)}{\cos \alpha_{1m}h} e^{\alpha_{1m}(x+b)}, \quad x \leq -b, \end{aligned}$$

$$(3.2b) \quad {}_1\zeta(x) = A_1 e^{-\alpha_{11}(x+b)} + \sum_{m=1}^{\infty} R_{1m} e^{\alpha_{1m}(x+b)}, \quad x \leq -b;$$

and in the downwave domain

$$(3.2c) \quad {}_1\phi = -\frac{ig}{\omega} \sum_{m=1}^{\infty} T_{1m} \frac{\cos \alpha_{1m}(z+h)}{\cos \alpha_{1m}h} e^{-\alpha_{1m}(x-b)}, \quad x \geq b,$$

$$(3.2d) \quad {}_1\zeta(x) = \sum_{m=1}^{\infty} T_{1m} e^{-\alpha_{1m}(x-b)}, \quad x \geq b,$$

where R_{11} and T_{11} are the amplitudes of the linear component of reflected and transmitted waves, respectively; R_{1m} and T_{1m} , $m = 2, 3, \dots$, are the amplitudes of the linear components of evanescent modes.

The eigenvalues must satisfy the following relations:

$$(3.2e) \quad \frac{\omega^2}{g} = -\alpha_{1m} \tan(\alpha_{1m}h), \quad m \geq 1,$$

where $\alpha_{1m} = \{-ik_1, \alpha_{12}, \alpha_{13}, \dots; k_1, \alpha_{12}, \dots > 0\}$.

In order to determine the coefficients of the eigenfunction expansions in (3.2), which are required to calculate free-surface elevations, it is convenient to introduce the velocity potential in the domain underneath the cylinder and apply matching conditions. The velocity potential in the fluid domain underneath the cylinder may be written in the form of the following eigenfunction expansions:

$$(3.3a) \quad {}_1\phi = -\frac{ig}{\omega} \sum_{m=1}^{\infty} [C_{1m}(1 - \delta_{1m} + \delta_{1m}x/b)e^{\mu_m x} + D_{1m}e^{-\mu_m x}] \\ \times \cos \mu_m(z+h), \quad |x| \leq b,$$

where

$$(3.3b) \quad \mu_m = \frac{(m-1)\pi}{h-d}, \quad m \geq 1.$$

The coefficients of the eigenfunction expansions can be quantified by applying matching conditions which impose the continuity of velocity potentials and their horizontal derivatives at $|x| = b$, $-h \leq z \leq -d$. Application of the latter boundary conditions results in formulas for the coefficients, R_{1m} and T_{1m}

$$(3.4) \quad R_{1m} = \delta_{1m}A_1 + \frac{4 \cos \alpha_{1m}h}{2\alpha_{1m}h + \sin 2\alpha_{1m}h} \sum_{l=1}^{\infty} [C_{1l}(\mu_l + \delta_{1l}/b)e^{-\mu_l b} - D_{1l}\mu_l e^{\mu_l b}] \\ \times \left[\frac{\sin(\mu_l - \alpha_{1m})(h-d)}{2(\mu_l - \alpha_{1m})} + \frac{\sin(\mu_l + \alpha_{1m})(h-d)}{2(\mu_l + \alpha_{1m})} \right], \quad m = 1, 2, \dots, \\ T_{1m} = -\frac{4 \cos \alpha_{1m}h}{2\alpha_{1m}h + \sin 2\alpha_{1m}h} \sum_{l=1}^{\infty} [C_{1l}(\mu_l + \delta_{1l}/b)e^{\mu_l b} - D_{1l}\mu_l e^{-\mu_l b}] \\ \times \left[\frac{\sin(\mu_l - \alpha_{1m})(h-d)}{2(\mu_l - \alpha_{1m})} + \frac{\sin(\mu_l + \alpha_{1m})(h-d)}{2(\mu_l + \alpha_{1m})} \right], \quad m = 1, 2, \dots$$

The coefficients C_{1m} and D_{1m} can be quantified in a similar manner from the condition of the continuity of velocity potentials at $|x| = b$.

A solution at second-order consists of a time-dependent and a time-independent part. In order to simplify the formulas for the velocity potential and free-surface elevations, it is convenient to introduce spatial function and separate a time-dependent factor at once. Accordingly, the nonlinear components of the solution can be expressed in the following form:

$$(3.5) \quad \begin{aligned} {}_2\Phi(x, z, t) &= \text{Re}[\mathcal{P}\phi(x, z)e^{-2i\omega t}] + {}_0^2\Phi(x, z) \\ {}_2\eta(x, t) &= \text{Re}[\mathcal{P}\zeta(x)e^{-2i\omega t}] + {}_0^2\eta(x), \end{aligned}$$

where the quantities in brackets are complex-valued spatial functions.

The time-independent solution is out of scope of the present studies. Accordingly, the nonlinear components of the velocity potential and free-surface elevation may be expressed as follows:

$$(3.6a) \quad \begin{aligned} {}_2\phi = & -\frac{ig}{2\omega} A_2 \frac{\cos \alpha_{21}(z+h)}{\cos \alpha_{21}h} e^{-\alpha_{21}(x+b)} \\ & -\frac{ig}{2\omega} \sum_{j=1}^{\infty} R_{2j} \frac{\cos \alpha_{2j}(z+h)}{\cos \alpha_{2j}h} e^{\alpha_{2j}(x+b)} \\ & -i\omega A_1^2 \frac{\alpha_{11}^2}{4\omega^4/g^2} \frac{6\omega^4/g^2 + 6\alpha_{11}^2}{4\omega^4/g^2} \frac{\cos 2\alpha_{11}(z+h)}{\cos^2 \alpha_{11}h} e^{-2\alpha_{11}(x+b)} \\ & + 2i\omega \sum_{m=1} A_1 R_{1m} \frac{\alpha_{11}\alpha_{1m}}{4\omega^4/g^2} \frac{6\omega^4/g^2 - 4\alpha_{11}\alpha_{1m} + \alpha_{1s}^2 + \alpha_{1m}^2}{4\omega^4/g^2 + (\alpha_{11} + \alpha_{1m})^2} \\ & \times \frac{\cos(\alpha_{11} - \alpha_{1m})(z+h)}{\cos \alpha_{11}h \cos \alpha_{1m}h} e^{-(\alpha_{11} - \alpha_{1m})(x+b)} \\ & -i\omega \sum_{s=1} \sum_{m=1} R_{1s} R_{1m} \frac{\alpha_{1s}\alpha_{1m}}{4\omega^4/g^2} \frac{6\omega^4/g^2 + 4\alpha_{1s}\alpha_{1m} + \alpha_{1s}^2 + \alpha_{1m}^2}{4\omega^4/g^2 + (\alpha_{1s} - \alpha_{1m})^2} \\ & \times \frac{\cos(\alpha_{1s} + \alpha_{1m})(z+h)}{\cos \alpha_{1s}h \cos \alpha_{1m}h} e^{(\alpha_{1s} + \alpha_{1m})(x+b)}, \end{aligned}$$

$$(3.6b) \quad \begin{aligned} {}_2\zeta(x) = & A_2 e^{-\alpha_{21}(x+b)} + \sum_{j=1}^{\infty} R_{2j} e^{\alpha_{2j}(x+b)} \\ & + \frac{g}{4\omega^2} A_1^2 \frac{\alpha_{11}^2 (\omega^4/g^2 + 3\alpha_{11}^2)}{\omega^4/g^2} e^{-2\alpha_{11}(x+b)} \\ & + \frac{g}{2\omega^2} \sum_{m=1}^{\infty} A_1 R_{1m} \frac{(\alpha_{11} - \alpha_{1m})^2 (\omega^4/g^2 - 3\alpha_{11}\alpha_{1m})}{4\omega^4/g^2 + (\alpha_{11} + \alpha_{1m})^2} e^{-(\alpha_{11} - \alpha_{1m})(x+b)} \\ & + \frac{g}{4\omega^2} \sum_{m=1}^{\infty} \sum_{s=1}^{\infty} R_{1m} R_{1s} \frac{(\alpha_{1m} + \alpha_{1s})^2 (\omega^4/g^2 + 3\alpha_{1m}\alpha_{1s})}{4\omega^4/g^2 + (\alpha_{1m} - \alpha_{1s})^2} e^{(\alpha_{1m} + \alpha_{1s})(x+b)}, \end{aligned}$$

for $x \leq -b$; and in the downwave area

$$(3.6c) \quad {}_2\phi = -\frac{ig}{2\omega} \sum_{j=1}^{\infty} T_{2j} \frac{\cos \alpha_{2j}(z+h)}{\cos \alpha_{2j}h} e^{-\alpha_{2j}(x-b)} \\ - i\omega \sum_{s=1}^{\infty} \sum_{m=1}^{\infty} T_{1s} T_{1m} \frac{\alpha_{1s}\alpha_{1m}}{4\omega^4/g^2} \frac{6\omega^4/g^2 + 4\alpha_{1s}\alpha_{1m} + \alpha_{1s}^2 + \alpha_{1m}^2}{4\omega^4/g^2 + (\alpha_{1s} - \alpha_{1m})^2} \\ \times \frac{\cos(\alpha_{1s} + \alpha_{1m})(z+h)}{\cos \alpha_{1s}h \cos \alpha_{1m}h} e^{-(\alpha_{1s} + \alpha_{1m})(x-b)},$$

$$(3.6d) \quad {}_2\zeta(x) = \sum_{j=1}^{\infty} T_{2j} e^{-\alpha_{2j}(x-b)} \\ + \frac{g}{4\omega^2} \sum_{m=1}^{\infty} \sum_{s=1}^{\infty} T_{1m} T_{1s} \frac{(\alpha_{1m} + \alpha_{1s})^2(\omega^4/g^2 + 3\alpha_{1m}\alpha_{1s})}{4\omega^4/g^2 + (\alpha_{1m} - \alpha_{1s})^2} \\ \times e^{-(\alpha_{1m} + \alpha_{1s})(x-b)},$$

for $x \geq b$, where A_2 is the amplitude of the nonlinear incoming wave, R_{21} and T_{21} are the amplitudes of the nonlinear component of reflected and transmitted waves, respectively; R_{2j} and T_{2j} , $j = 2, 3, \dots$, are the amplitudes of the nonlinear components of evanescent modes.

The eigenvalues of the nonlinear solution must satisfy the following relations:

$$(3.6e) \quad \frac{4\omega^2}{g} = -\alpha_{2j} \tan \alpha_{2j}h, \quad j \geq 1,$$

where $\alpha_{2j} = \{-ik_2, \alpha_{22}, \alpha_{23}, \dots; k_2, \alpha_{22}, \dots > 0\}$.

In order to determine the coefficients of the eigenfunction expansions in (3.6), which are required to calculate the nonlinear components of the free-surface elevations, it is convenient to introduce the velocity potential in the domain underneath the cylinder and apply matching conditions. The second-order velocity potential in the fluid domain underneath the cylinder may be written in the following form:

$$(3.7) \quad {}_2\phi = -\frac{ig}{2\omega} \sum_{j=1}^{\infty} [C_{2j}(1 - \delta_{1j} + \delta_{1j}x/b)e^{\mu_j x} + D_{2j}e^{-\mu_j x}] \\ \times \cos \mu_j(z+h), \quad |x| \leq b.$$

The coefficients of the eigenfunction expansions at second order can be quantified by applying matching conditions which impose the continuity of velocity potentials and their horizontal derivatives at $|x| = b$, $-h \leq z \leq -d$. Application of the latter boundary conditions results in formulas for the coefficients, R_{2j} and T_{2j}

$$(3.8a) \quad R_{2j} = \delta_{1j}A_2 + \frac{4 \cos \alpha_{2j}h}{2\alpha_{2j}h + \sin 2\alpha_{2j}h} \left\{ \sum_{l=1} [C_{2l}(\mu_l + \delta_{1l}/b)e^{-\mu_l b} - D_{2l}\mu_l e^{\mu_l b}] \right. \\ \left. \times \left[\frac{\sin(\mu_l - \alpha_{2j})(h-d)}{2(\mu_l - \alpha_{2j})} + \frac{\sin(\mu_l + \alpha_{2j})(h-d)}{2(\mu_l + \alpha_{2j})} \right] + S_{Rj} \right\}, \quad j = 1, 2, \dots,$$

$$(3.8b) \quad T_{2j} = -\frac{\cos \alpha_{2j}h}{2\alpha_{2j}h + \sin 2\alpha_{2j}h} \left\{ \sum_{l=1} [C_{2l}(\mu_l + \delta_{1l}/b)e^{\mu_l b} - D_{2l}\mu_l e^{-\mu_l b}] \right. \\ \left. \times \left[\frac{\sin(\mu_l - \alpha_{2j})(h-d)}{2(\mu_l - \alpha_{2j})} + \frac{\sin(\mu_l + \alpha_{2j})(h-d)}{2(\mu_l + \alpha_{2j})} \right] + S_{Tj} \right\}, \quad j = 1, 2, \dots,$$

where

$$(3.8c) \quad S_{Rj} = 2\frac{\omega^2}{g}A_1^2 \frac{\alpha_{11}}{\cos^2 \alpha_{11}h} \frac{\alpha_{11}^2}{4\omega^4/g^2} \frac{6\omega^4/g^2 + 6\alpha_{11}^2}{4\omega^4/g^2} \\ \times \left[\frac{\sin(2\alpha_{11} - \alpha_{2j})h}{2\alpha_{11} - \alpha_{2j}} + \frac{\sin(2\alpha_{11} + \alpha_{2j})h}{2\alpha_{11} + \alpha_{2j}} \right] \\ + 2\frac{\omega^2}{g} \sum_{m=1} A_1 R_{1m} \frac{\alpha_{11} - \alpha_{1m}}{\cos^2 \alpha_{11}h \cos \alpha_{1m}h} \frac{\alpha_{11}\alpha_{1m}}{4\omega^4/g^2} \frac{6\omega^4/g^2 - 4\alpha_{11}\alpha_{1m} + \alpha_{1s}^2 + \alpha_{1m}^2}{4\omega^4/g^2 + (\alpha_{11} + \alpha_{1m})^2} \\ \times \left[\frac{\sin(\alpha_{11} - \alpha_{1m} - \alpha_{2j})h}{\alpha_{11} - \alpha_{1m} - \alpha_{2j}} + \frac{\sin(\alpha_{11} - \alpha_{1m} + \alpha_{2j})h}{\alpha_{11} - \alpha_{1m} + \alpha_{2j}} \right] \\ - \frac{\omega^2}{g} \sum_{m=1} \sum_{s=1} R_{1m} R_{1s} \frac{\alpha_{1m} + \alpha_{1s}}{\cos \alpha_{1m}h \cos \alpha_{1s}h} \frac{\alpha_{1s}\alpha_{1m}}{4\omega^4/g^2} \frac{6\omega^4/g^2 + 4\alpha_{1s}\alpha_{1m} + \alpha_{1s}^2 + \alpha_{1m}^2}{4\omega^4/g^2 + (\alpha_{1s} - \alpha_{1m})^2} \\ \times \left[\frac{\sin(\alpha_{1m} + \alpha_{sm} - \alpha_{2j})h}{\alpha_{1m} + \alpha_{1s} - \alpha_{2j}} + \frac{\sin(\alpha_{1m} + \alpha_{1s} + \alpha_{2j})h}{\alpha_{1m} + \alpha_{1s} + \alpha_{2j}} \right],$$

$$(3.8d) \quad S_{Tj} = \frac{\omega^2}{g} \sum_{m=1} \sum_{s=1} T_{1m} T_{1s} \frac{\alpha_{1m} + \alpha_{1s}}{\cos \alpha_{1m}h \cos \alpha_{1s}h} \frac{\alpha_{1s}\alpha_{1m}}{4\omega^4/g^2} \\ \times \frac{6\omega^4/g^2 + 4\alpha_{1s}\alpha_{1m} + \alpha_{1s}^2 + \alpha_{1m}^2}{4\omega^4/g^2 + (\alpha_{1s} - \alpha_{1m})^2} \\ \times \left[\frac{\sin(\alpha_{1m} + \alpha_{sm} - \alpha_{2j})h}{\alpha_{1m} + \alpha_{1s} - \alpha_{2j}} + \frac{\sin(\alpha_{1m} + \alpha_{1s} + \alpha_{2j})h}{\alpha_{1m} + \alpha_{1s} + \alpha_{2j}} \right].$$

The coefficients C_{2j} and D_{2j} can be quantified in a similar manner from the condition of the continuity of the second-order velocity potentials at $|x| = b$.

The linear component of the free-surface elevation ${}_1\zeta(x)$ consists of standard modes, e.g., progressive waves and evanescent modes. The nonlinear component of the free-surface elevation ${}_2\zeta(x)$ is far more complex and consists of

near- and far-field parts. The near-field part is due to second-order evanescent modes ($j > 1$) as well as first-order wave-evanescent mode and evanescent mode-evanescent mode interactions. The far-field part is due to second-order free-waves ($j = 1$) and first-order wave-wave interaction and, which is interesting to note, does not contain a product of the interaction between two first-order waves propagating in the opposite directions. In the classical derivation of the nonlinear component of the free-surface elevation, in which only one propagating wave is considered, a product of the first-order wave-wave interaction is called the Stokes wave. The above formula is the result of an extension of the classical derivation as a general first-order potential was taken into consideration.

3.2. Far-field components

The linear components of the velocity potential and free-surface elevation are described in terms of eigenfunction expansions by simple, standard forms which are typically applied to describe wave-structure interaction problems [12, 19]. The formulas derived for the nonlinear component of the time-dependent part of the velocity potential and free-surface elevation, Eqs. (3.6a)–(3.6d) possess complex forms which are the result of the interaction between various first-order modes. The complexities of the formulas are mainly due to evanescent modes. Far away from a disturbance, where the evanescent modes can be practically neglected, the nonlinear components of the velocity potential and free-surface elevation are determined by simple expressions that may be analyzed easier. Namely, the nonlinear components of the velocity potential and the free-surface elevation far away from the cylinder are

$$(3.9a) \quad \begin{aligned} {}_2\phi(x, z) = & -\frac{ig}{2\omega}A_2\frac{\cosh k_2(z+h)}{\cosh k_2h}e^{ik_2(x+b)} \\ & -\frac{ig}{2\omega}R_{21}\frac{\cosh k_2(z+h)}{\cosh k_2h}e^{-ik_2(x+b)} \\ & -\frac{3}{8}i\omega A_1^2\frac{\cosh 2k_1(z+h)}{\sinh^4 k_1h}e^{2ik_1(x+b)} + \frac{1}{4}i\omega A_1R_{11}\left(3 + \frac{g^2}{\omega^4}k_1^2\right) \\ & -\frac{3}{8}i\omega R_{11}^2\frac{\cosh 2k_1(z+h)}{\sinh^4 k_1h}e^{-2ik_1(x+b)}, \quad x \rightarrow -\infty, \end{aligned}$$

$$(3.9b) \quad \begin{aligned} {}_2\zeta(x) = & A_2e^{ik_2(x+b)} + R_{21}e^{-ik_2(x+b)} \\ & + \frac{1}{4}A_1^2k_1\frac{\cosh k_1h}{\sinh^3 k_1h}(2 + \cosh 2k_1h)e^{2ik_1(x+b)} \\ & + \frac{1}{4}R_{11}^2k_1\frac{\cosh k_1h}{\sinh^3 k_1h}(2 + \cosh 2k_1h)e^{-2ik_1(x+b)}, \quad x \rightarrow -\infty; \end{aligned}$$

and in the downwave domain

$$(3.9c) \quad {}_2\phi(x, z) = -\frac{ig}{2\omega} T_{21} \frac{\cosh k_2(z+h)}{\cosh k_2 h} e^{ik_2(x-b)} \\ - \frac{3}{8} i\omega T_{11}^2 \frac{\cosh 2k_1(z+h)}{\sinh^4 k_1 h} e^{2ik_1(x-b)}, \quad x \rightarrow \infty,$$

$$(3.9d) \quad {}_2\zeta(x) = T_{21} e^{ik_2(x-b)} \\ + \frac{1}{4} T_{11}^2 k_1 \frac{\cosh k_1 h}{\sinh^3 k_1 h} (2 + \cosh 2k_1 h) e^{2ik_1(x-b)}, \quad x \rightarrow \infty.$$

The first two terms in Eq. (3.9b) represent the right- and left-progressing free-waves, while the remaining two terms represent the right- and left-progressing Stokes waves of amplitudes A_{2S} and R_{2S} , respectively. On the downwave side, the first term in Eq. (3.9d) represents the right-progressing free-waves, while the second term represents the right-progressing Stokes wave of amplitude T_{2S} . The amplitudes of Stokes waves can be determined from Eqs. (3.9b) and (3.9d). Accordingly, on the upwave side of the cylinder the amplitudes of the Stokes waves can be written in the following form:

$$(3.10a) \quad A_{2S} = \frac{1}{4} A_1^2 k_1 \frac{\cosh k_1 h}{\sinh^3 k_1 h} (2 + \cosh 2k_1 h),$$

$$(3.10b) \quad R_{2S} = \frac{1}{4} |R_{11}^2| k_1 \frac{\cosh k_1 h}{\sinh^3 k_1 h} (2 + \cosh 2k_1 h);$$

and on the downwave side the cylinder the amplitude of the Stokes wave is

$$(3.10c) \quad T_{2S} = \frac{1}{4} |T_{11}^2| k_1 \frac{\cosh k_1 h}{\sinh^3 k_1 h} (2 + \cosh 2k_1 h).$$

It is worth noting that the second-order free-waves travel with a speed of $2\omega/k_2$, while the Stokes wave travels with a speed of ω/k_1 . Since $k_2 > 2k_1$, the nonlinear free-waves travel at a speed that is slower than the Stokes wave. There are many consequences of the above phenomena. The most publicized seems to be the generation of waves of nonpermanent form by a sinusoidally moving wavemaker in a 2D wave flume. It is also interesting to note that a constant term associated with the interaction between the linear component of left- and right-progressing waves, that was expected to appear in the formula for ${}_2\zeta(x)$ due to the form of Eq. (3.9a), has been canceled in Eq. (3.9b). It is also evident from Eqs. (3.9b) and (3.9d) that the linear components of evanescent modes do not directly contribute to ${}_2\zeta(x)$ far away from the cylinder. However, the linear components of evanescent modes may indirectly contribute to ${}_2\zeta(x)$ by contributing to R_{21} or to T_{21} , or to both amplitudes.

The derived solution satisfies all boundary conditions including radiation conditions. The solution is relatively general and can be applied to describe a nonlinear wave diffraction or radiation problem for a cylinder of an arbitrary cross-section. This can be achieved by applying Eqs. (3.2) and (3.6) in a hybrid model, which enables us to derive a nonlinear solution for a cylinder of an arbitrary cross-section. Moreover, Eqs. (3.2) and (3.6) can be directly applied to solve the wavemaker problem and a variety of cases for wave radiation or diffraction by a horizontal rectangular cylinder for which the coefficients in Eqs. (3.2) and (3.6) can be determined analytically or by the method of matched eigenfunction expansions.

4. Results

The derived solution was applied to calculate reflection and transmission of nonlinear water waves at a semi-submerged dock. The nonlinear components of water waves on the upwave and downwave sides of the dock are analyzed for the wide range of wave frequencies and two basic geometric parameters of the model, e.g., dock width and draft. The results are made dimensionless and are plotted as a function of the dimensionless wave number $k_1 h$.

The width of a dock is one of the two main geometric parameters for the problem of nonlinear wave interaction with a horizontal rectangular dock. The effect of a dock width on nonlinear components of free-surface elevation is presented in Fig. 2. The plots present the amplitudes of the nonlinear components of the free-surface elevation (R_{21}) and (T_{21}) for two dock widths, $b/h = 0.4$ and $b/h = 0.6$. In order to show the values of the results in shallow water and to obtain dimensionless quantities independent on the amplitude of the incident wave, R_{21} and T_{21} are divided by the amplitude of the incoming Stokes waves.

The plots presented in Fig. 2 show that the width of a dock has a significant effect on the reflection and transmission of nonlinear waves at a semi-submerged dock. The results show that the reflection of nonlinear waves increases with increasing dock width for shallow water waves and decreases with increasing dock width for intermediate- and deep-water waves. A similar tendency indicates wave transmission, namely, the transmission of nonlinear waves increases with increasing dock width for shallow water waves and decreases with increasing dock width for intermediate- and deep-water waves. The phenomenon of the simultaneous increase or decrease of the reflection and transmission of nonlinear waves is an interesting result. In general, wave reflection is expected to increase when wave transmission decreases and vice versa; however, the results show that wave reflection and transmission simultaneously increases or decreases with increasing the dock width. This outcome arises from the complexity of a nonlinear diffraction problem. One needs to realize that a second-order solution arises

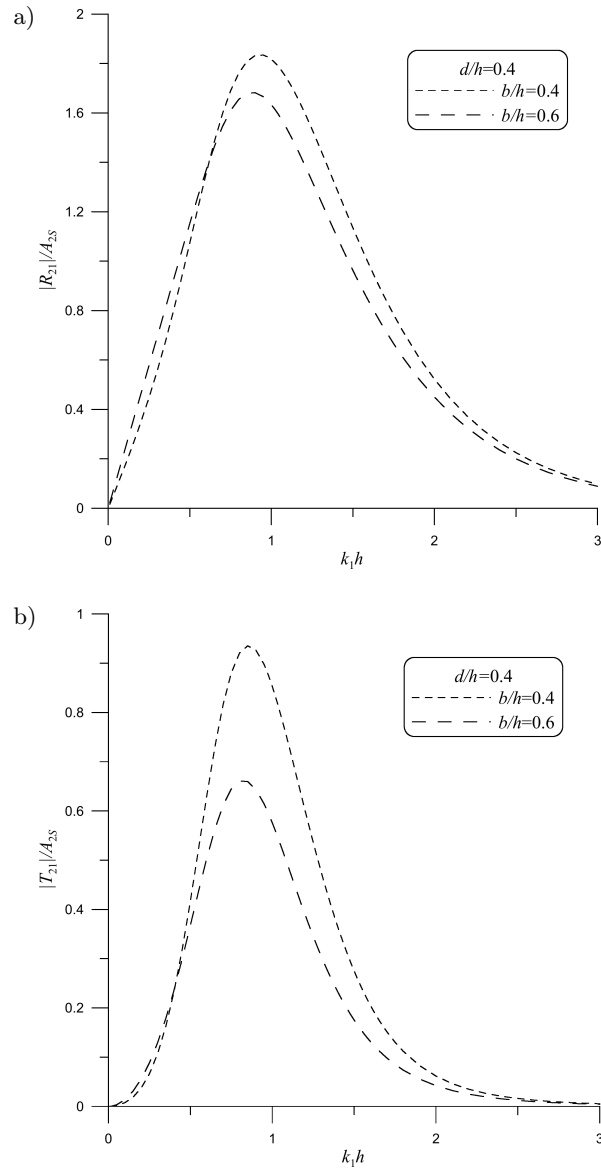


FIG. 2. Effect of dock width on the amplitudes of the nonlinear reflected and transmitted waves: a) reflected waves, b) transmitted waves.

from higher-order products of first-order waves as well as from a contribution of second-order waves. As a consequence, higher-order products are affected by various functions of $k_1 h$ and $k_2 h$, which are governed by different dispersion relations and cannot be simplified as in the case of linear wave theory.

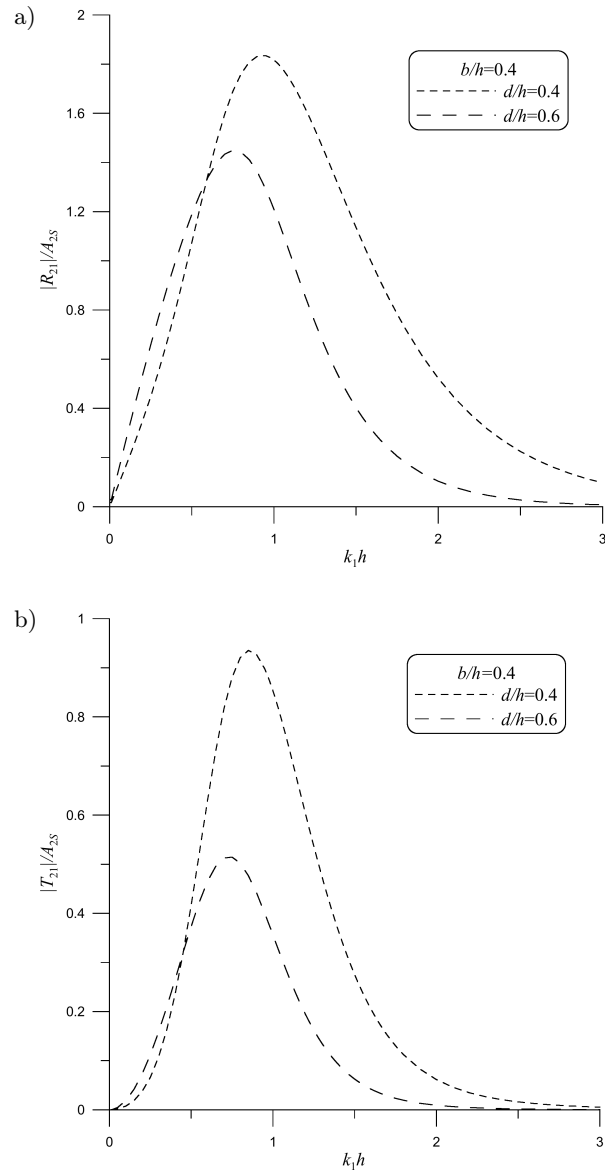


FIG. 3. Effect of dock draft on the amplitudes of the nonlinear reflected and transmitted waves: a) reflected waves, b) transmitted waves.

The draft of the dock is the second geometric parameter for the problem of the nonlinear wave interaction with a horizontal rectangular dock. The effect of the draft of the dock on nonlinear components of free-surface elevation is shown in Fig. 3. The plots present the amplitudes of the nonlinear components

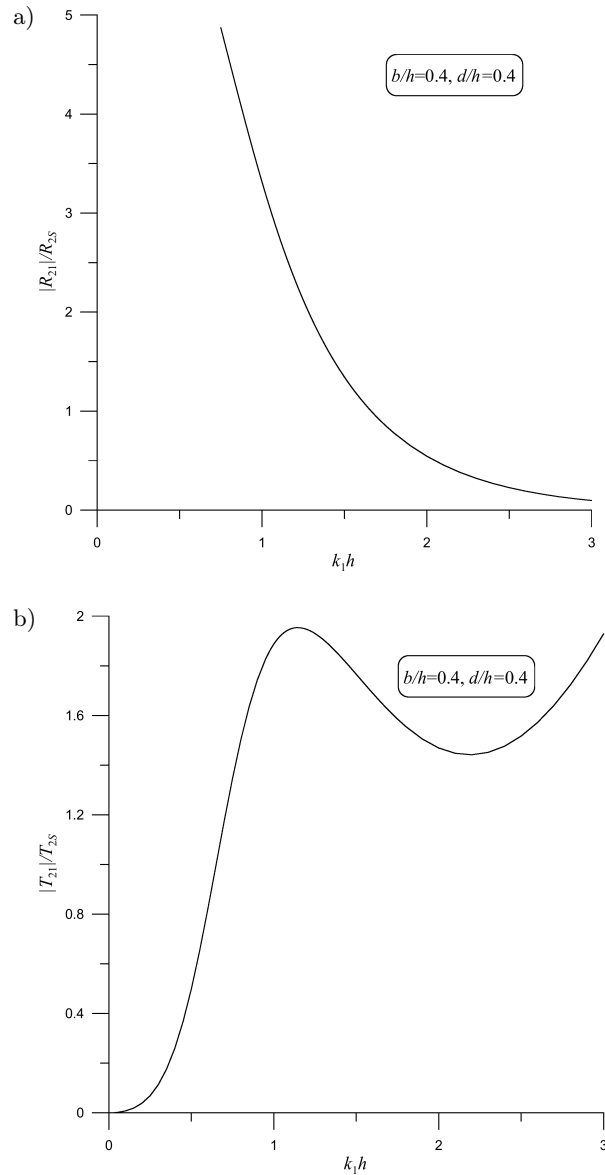


FIG. 4. Ratio of the amplitudes of the nonlinear reflected and transmitted waves to the amplitudes of the corresponding nonlinear Stokes waves: a) reflected waves, b) transmitted waves.

of the free-surface elevation (R_{21}) and (T_{21}) for two dock drafts, $d/h = 0.4$ and $d/h = 0.6$. The results plotted in Fig. 3 are dimensionless.

The plots in Fig. 3 show that the draft of a dock has a significant effect on the reflection and transmission of nonlinear waves at a semi-submerged dock.

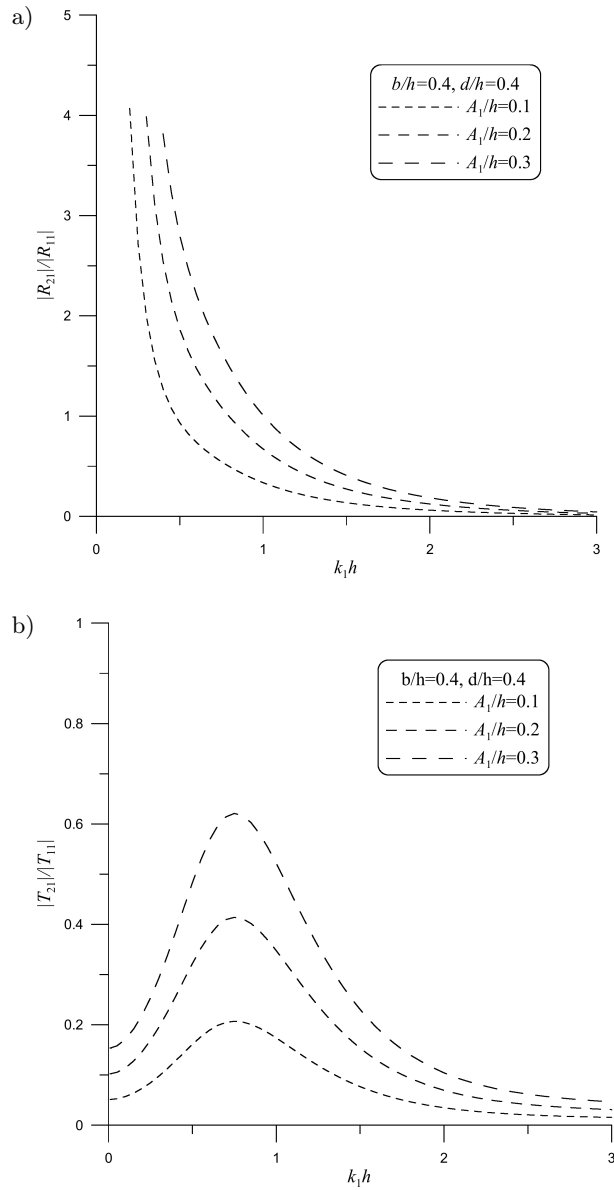


FIG. 5. Ratio of the amplitudes of nonlinear reflected and transmitted waves to the amplitudes of the corresponding linear waves: a) reflected waves, b) transmitted waves.

The results show that the reflection of nonlinear waves increases with increasing dock draft for shallow water waves and decreases with increasing dock draft for intermediate- and deep-water waves. A similar tendency indicates wave transmission, namely, the transmission of nonlinear waves increases with increasing

dock draft for shallow water waves and decreases with increasing dock draft for intermediate- and deep-water waves. This result is interesting because wave reflection is expected to increase when wave transmission decreases and vice versa. However, the results show that wave reflection and transmission simultaneously increase or decrease with increasing the draft of the dock, which is a noteworthy outcome.

An analysis indicates that nonlinear reflected and transmitted waves generated due to the interaction of water waves with a dock provide a significant contribution to the total diffracted wave field. This demonstrates the results of the ratio of the amplitudes of the nonlinear component of the free-surface elevation (R_{21}, T_{21}) to the amplitudes of the corresponding second-order Stokes waves plotted in Fig. 4. The results show that the nonlinear components of the reflected and transmitted free-waves may exceed many times the amplitudes of the corresponding second-order Stokes waves. Especially high are the nonlinear waves on the upwave side of the dock. The analysis shows that the nonlinear reflected and transmitted waves may provide a dominant contribution to the total wave field, which demonstrates the plots of the ratio of the amplitudes of the nonlinear reflected (R_{21}) and transmitted (T_{21}) waves to the amplitudes of the corresponding linear components presented in Fig. 5. The plots show that the nonlinear waves may become the dominant contributions to the wave field for a wide range of wave frequencies. A detailed analysis indicates that the nonlinear wave components may exceed the amplitudes of the corresponding linear waves within commonly accepted range of the applicability of the weakly nonlinear wave theory. This conclusion is of significant importance for many problems of practical importance, including a sediment transport, for which second-order waves have been shown to be the main driving force [20, 21].

5. Experiments

5.1. Laboratory experiments

Laboratory experiments were conducted in the wave flume at the Chalmers University of Technology in Göteborg to verify the present theory. The wave flume is 80 m long, 2 m wide and 1 m deep. It is equipped with a movable hinge wave generator. A wave absorbing slope is supplied at the end of the wave flume.

A rectangular dock was built in the middle part of the wave flume. The dock was built as a beam frame covered with walls of PVC. The draft of the dock was $d = 0.3$ m and the beam $2b = 0.61$ m. The water depth in the wave flume was $h = 0.4$ m. A group of two resistance-type wave gauges was located in front of the dock to measure the free-surface elevation and a similar group of wave gauges was used to measure the free-surface elevation on the downwave side.

The dock was exposed to plane waves generated by a sinusoidally moving wave-maker. Water waves were generated for four wave steepnesses to investigate the effect of wave steepness on nonlinear wave reflection and transmission. Waves of higher steepness were achieved by increasing the amplitude of wavemaker oscillations. The measurements were conducted after the steady-state conditions were established in the wave flume, but before re-reflection disturbed the measurements.

The free-surface elevation was recorded during four wave periods. The measurements were sampled 64 times per wave period, so one measured record contained 256 samples. This approach made it possible to see if the measured quantities remain stable for consecutive waves. Moreover, the leakage problem associated with the application of the Fourier analysis was also avoided since the number of samples is an integer power of two.

5.2. Comparisons with experiments

The analysis of the nonlinear wave field in the wave flume is a complex task. This is a consequence of complex reflections of different wave components, nonlinear wave interactions, and various side effects. The analysis of the free-surface elevation and the separation of the incident, reflected, and transmitted wave trains were conducted by adapting the multi-gauge method [22, 23] to the problem of the separation of nonlinear incident and reflected waves. The method is extended here to calculate linear and nonlinear components of water waves in the wave flume including the amplitudes and phases of the incident, reflected and transmitted waves. The derived experimental quantities were used to conduct verification of the theoretical approach.

In order to calculate linear and nonlinear components of water waves in a wave train and to separate incoming and reflected waves, M_1 wave gauges are selected on the upwave side of the dock at $(x_m, 0)$, $m = 1, \dots, M_1$, and M_2 wave gauges are selected on the downwave side of the dock at $(x_m, 0)$, $m = M_1 + 1, \dots, M_1 + M_2$. By applying the multi-gauge method, the amplitude of the incoming (A_n), reflected (R_{n1}), and transmitted (T_{n1}), waves can be computed from

$$(5.1a) \quad A_n = \frac{\sum_{m=1}^{M_1} e^{-2ik_n x_m} \sum_{m=1}^{M_1} c_{nm} e^{ik_n x_m} - M_1 \sum_{m=1}^{M_1} c_{nm} e^{-ik_n x_m}}{\sum_{m=1}^{M_1} e^{-2ik_n x_m} \sum_{m=1}^{M_1} e^{2ik_n x_m} - M_1^2},$$

$$(5.1b) \quad R_{n1} = \frac{\sum_{m=1}^{M_1} e^{2ik_n x_m} \sum_{m=1}^{M_1} c_{nm} e^{-ik_n x_m} - M_1 \sum_{m=1}^{M_1} c_{nm} e^{ik_n x_m}}{\sum_{m=1}^{M_1} e^{-2ik_n x_m} \sum_{m=1}^{M_1} e^{2ik_n x_m} - M_1^2},$$

$$(5.1c) \quad T_{n1} = \frac{\sum_{m=M_1+1}^{M_1+M_2} e^{-2ik_n x_m} \sum_{m=M_1+1}^{M_1+M_2} c_{nm} e^{ik_n x_m} - M_2 \sum_{m=M_1+1}^{M_1+M_2} c_{nm} e^{-ik_n x_m}}{\sum_{m=M_1+1}^{M_1+M_2} e^{-2ik_n x_m} \sum_{m=M_1+1}^{M_1+M_2} e^{2ik_n x_m} - M_2^2},$$

where c_{nm} is the complex-valued amplitude of Fourier series component corresponding to wave frequency $n\omega$.

The linear component of reflected and transmitted wave amplitudes can be calculated by a standard application of Eq. (5.1) in a similar manner as in Sulisz [24, 25]. However, the determination of the nonlinear components of wave reflection and transmission requires a nonstandard approach. The problem is that the amplitudes of Fourier series component corresponding to wave frequency 2ω , i.e., c_{2m} , contain the product of second-order Stokes waves as well as second-order free-waves generated by the wavemaker [23]. It is necessary to subtract the contributions of these waves on the upwave and downwave side of the dock to obtain the nonlinear components of free reflected and transmitted waves for comparisons with theoretical results. The contributions of second-order incoming, reflected, and transmitted Stokes waves are calculated by applying measured first-order wave amplitudes as well as nonlinear Stokes wave theory and are deducted from c_{2m} with proper phases. This enables us to calculate the second-order free-wave generated by the wavemaker and subtract its contribution from c_{2m} to obtain the nonlinear components of free reflected and transmitted waves for comparisons with theoretical results. The described procedure illustrates the complexity of the derivation of the amplitudes of reflected and transmitted waves at second order. The procedure is far more complex when orders higher than two are considered because the product of nonlinear wave interactions and wave numbers involve unknown amplitudes.

The theoretical results and experimental data for nonlinear components of reflected and transmitted waves are shown in Fig. 6 and Fig. 7. The plots in Fig. 6 present the second-order components of the reflected and transmitted free-waves and the plots in Fig. 7 show the corresponding amplitudes of the second-order Stokes waves. The comparisons are conducted for four sequences of the laboratory waves generated with subsequent wavemaker amplitudes. The results plotted in Fig. 6 and Fig. 7 are dimensional (SI).

The plots in Fig. 6 and Fig. 7 show that the theoretical results are in reasonable agreement with the experimental data. A fairly good agreement between the theoretical results and experimental data is observed for four wave trains considered in laboratory experiments. It is interesting to notice that a reasonable agreement is observed between the theoretical results and experimental data on the upwave and downwave sides of the dock. The discrepancies between theoretical results and corresponding experimental data observed on the downwave

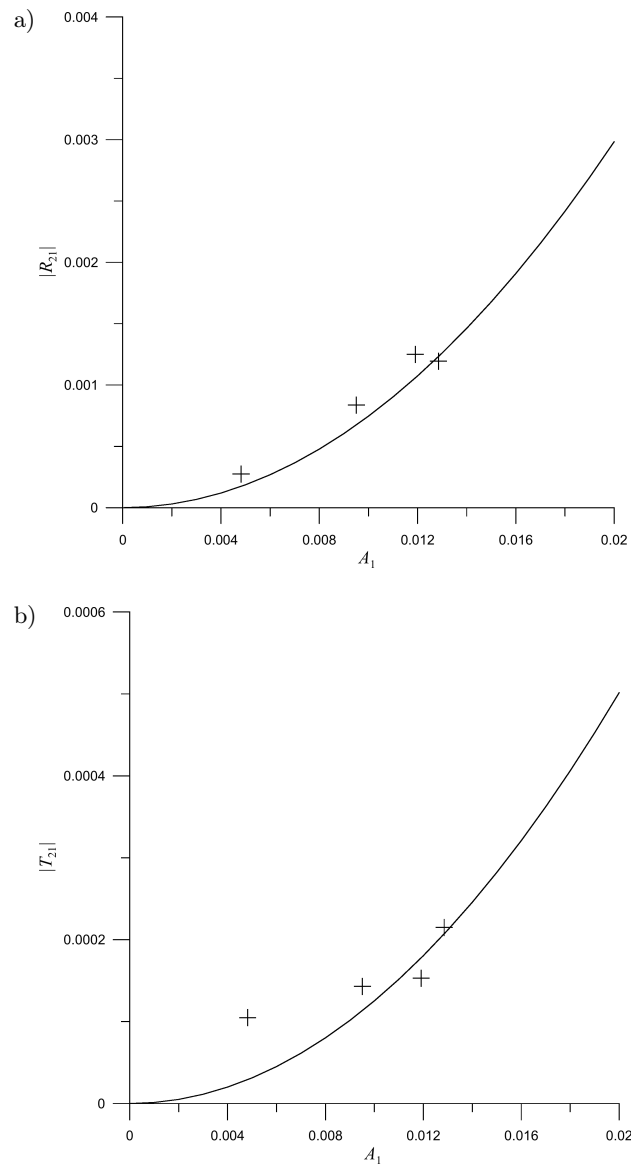


FIG. 6. Theoretical results (—) and experimental data (+) of the amplitudes of the nonlinear reflected and transmitted waves, $b/h = 0.7625$, $d/h = 0.75$, $k_1 h = 0.5$: a) reflected waves, b) transmitted waves.

sides for the wave sequence of the lowest amplitude are probably due to the measurements of the unsteady waves. The analysis of four subsequent waves in the recorded wave train indicates that in this particular case a steady-state condition were not fully established on the downwave side of the dock before

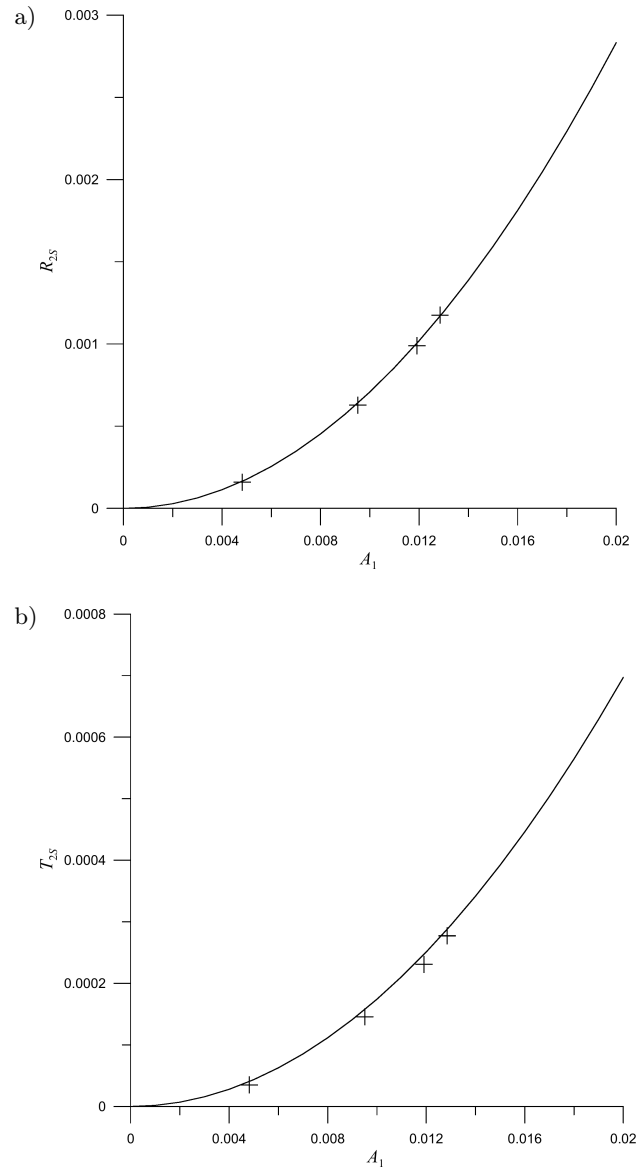


FIG. 7. Theoretical results (—) and experimental data (+) of the amplitudes of the nonlinear reflected and transmitted Stokes waves, $b/h=0.7625$, $d/h=0.75$, $k_1h=0.5$: a) reflected waves, b) transmitted waves.

the measurement started. There is often a problem with recording steady-state nonlinear waves in a relatively short wave flume because nonlinear wave components, due to a slower speed, require more time to reach a steady-state condition and the recording has to be terminated before re-reflection disturbed the mea-

surements. This probably caused observed discrepancies because, for waves of higher steepness, the comparison between theoretical results and experimental data is satisfactory.

6. Summary

A theoretical approach is applied to predict reflection and transmission of nonlinear water waves at a semi-submerged dock. The solution for the dock of arbitrary draft was achieved analytically and by the method of matched eigenfunction expansions. The solution was applied to calculate nonlinear wave field scattered by the dock and focus on nonlinear components of wave reflection and transmission arising from the interaction of water waves with the dock.

The results show that the dock geometry has a significant effect on the nonlinear components of wave reflection and transmission. The reflection and transmission of nonlinear waves increase with increasing dock width for shallow water waves and decrease with increasing dock width for intermediate- and deep-water waves. A similar tendency indicates wave reflection and transmission with respect to the changes of the dock draft, namely, the reflection and transmission of nonlinear waves increases with increasing dock draft for shallow water waves and decreases with increasing dock draft for intermediate- and deep-water waves. The results are novel and noteworthy because wave reflection and transmission simultaneously increase or decrease with the changes of the dock geometry. In general, wave reflection is expected to increase when wave transmission decreases and vice versa. This surprising outcome arises from the complexity of the nonlinear diffraction problem.

The solution reveals that the scattered components of nonlinear reflected and transmitted waves may provide a significant contribution to the wave field for a wide range of wave and dock parameters. The results show that the nonlinear components of reflected and transmitted waves may exceed many times the amplitudes of the corresponding second-order Stokes waves. The nonlinear reflected waves may also exceed many times corresponding linear components for a wide range of wave frequencies. These phenomena occur within the commonly accepted range of the applicability of a second-order wave theory and imply a need to include scattered components of nonlinear free-surface elevation in the analysis of many problems of practical importance, including a sediment transport, for which second-order waves have been shown to be the main driving force.

A special effort was devoted to laboratory experiments and accompanying procedures because the verification required a separation of several components of the same frequency and standard decomposition methods could not be applied. The second-order components of the reflected and transmitted free-waves and Stokes waves were compared with corresponding experimental data for waves of

different steepness. The comparisons show that theoretical results are in reasonable agreement with experimental data.

Acknowledgement

Financial support for this study was provided by the Institute of Hydroengineering, Polish Academy of Sciences, Gdańsk.

References

1. J.J. STOKER, *Water Waves*, Interscience Publishers, New York, 1957.
2. K. TAKANO, *The effects of a rectangular obstacle on wave propagation*, *La Houille Blanche*, **15**, 3, 247–259, 1960.
3. P. MCIVER, *Wave forces on adjacent floating bridge*, *Applied Ocean Research*, **8**, 2, 67–75, 1986.
4. W. SULISZ, W.G. MCDUGAL, *Wave interaction with a composite breakwater*, Proceedings of the International Conference on Computer Modeling in Ocean Engineering, A.A. Balkema, Rotterdam, The Netherlands, 715–721, 1988.
5. C.C. MEI, J.L. BLACK, *Scattering of surface waves by rectangular obstacles in waters of finite depth*, *Journal of Fluid Mechanics*, **38**, 3, 499–511, 1969.
6. J.L. BLACK, C.C. MEI, M.C.G. BRAY, *Radiation and scattering of water waves by rigid bodies*, *Journal of Fluid Mechanics*, **46**, 1, 151–164, 1971.
7. B. LE MEHAUTE, *Permeability of rubble-mound breakwaters for periodic gravity waves*, *La Houille Blanche*, **6**, 903–919, 1957.
8. K.J. BAI, R.W. YEUNG, *Numerical solutions to free-surface flow problems*, Proc. Tenth Naval Hydrodynamics Symposium, Cambridge, MA, 609–633, 1974.
9. K. J. BAI, *Diffraction of oblique waves by an infinite cylinder*, *Journal of Fluid Mechanics*, **68**, 3, 513–535, 1975.
10. W.G. MCDUGAL, W. SULISZ, *Seabed stability near floating structures. Journal of Waterway, Port, Coastal and Ocean Engineering*, ASCE, **115**, 6, 727–739, 1989.
11. W. SULISZ, M. JOHANSSON, *Second-order wave loading on a horizontal rectangular cylinder of substantial draught*, *Applied Ocean Research*, **14**, 333–340, 1992.
12. W. SULISZ, *Wave loads on caisson founded on multilayered rubble base*, *Journal of Waterway, Port, Coastal and Ocean Engineering*, ASCE, **123**, 3, 91–101, 1997.
13. H.O. FALTINSEN, E.A. LØKENØ, *Slow drift oscillations of a ship in irregular waves*, *Applied Ocean Research*, **1**, 1, 21–31, 1979.
14. W. SULISZ, *Diffraction of second-order surface waves by semi-submerged horizontal rectangular cylinder*, *Journal of Waterway, Port, Coastal, and Ocean Engineering*, ASCE, **119**, 2, 160–171, 1993.
15. W. LI, N. WILLIAMS, *The diffraction of second-order bichromatic waves by a semi-immersed horizontal rectangular cylinder*, *Journal of Fluid and Structures*, **13**, 381–397, 1999.

16. W. SULISZ, *Nonlinear wave diffraction problem for a rectangular obstacle*. Chapter 4, Non-linear Water Wave Interaction, Mahrenholtz & M. Markiewicz [eds.], International Series on Advances in Fluid Mechanics, Computational Mechanics Publications, Southampton, 1999.
17. J.V. WEHAUSEN, *Surface Waves*, [in:] Handbuch der Physik, 9, Springer, Berlin, 446–778, 1960.
18. W. SULISZ, M. PAPROTA, *Modeling of the propagation and evolution of nonlinear waves in a wave train*, Archives of Mechanics, **63**, 3, 311–335, 2011.
19. W. SULISZ, W.G. MCDUGAL, C.K. SOLLITT, *Water wave interaction with rubble toe protection*, Ocean Engineering, **16**, 5/6, 463–473, 1989.
20. J.A. BAILARD, *An energetic total load sediment transport model for a plane sloping beach*, Journal of Geophysical Research, **86**, c11, 10938–10954, 1981.
21. J.S. RIBBERINK, *Bed-load transport for steady flows and unsteady oscillatory flows*, Coastal Engineering, **34**, 1-2, 59–82, 1998.
22. P. JOLAS, *Contribution to the study of periodic oscillations of fluids with a free surface*, La Houille Blanche, **6**, 758–769, 1962.
23. W. SULISZ, R.T. HUDSPETH, *Complete second-order solution for water waves generated in wave flumes*, Journal of Fluid and Structures, **7**, 253–268, 1993.
24. W. SULISZ, *Wave propagation in channel with side porous caves*, Journal of Waterway, Port, Coastal, and Ocean Engineering, ASCE, **131**, 4, 162–170, 205.
25. W. SULISZ, *Diffraction of water waves by a semi-submerged structure in a channel*, Journal of Waterway, Port, Coastal, and Ocean Engineering, ASCE, **137**, 6, 269–280, 2011.

Received February 29, 2012; revised version April 10, 2013.
